AIP Advances

Transfer of a levitating nanoparticle between optical tweezers

Cite as: AIP Advances **11**, 025246 (2021); https://doi.org/10.1063/5.0024432
Submitted: 07 August 2020 . Accepted: 26 October 2020 . Published Online: 23 February 2021

M. Calamai, A. Ranfagni, and F. Marin

Transfer of a levitating nanoparticle between optical tweezers

Cite as: AIP Advances 11, 025246 (2021); doi: 10.1063/5.0024432
Submitted: 7 August 2020 • Accepted: 26 October 2020 •
Published Online: 23 February 2021

M. Calamai,[1] A. Ranfagni,[1,2] and F. Marin[1,2,3,4,a)]

AFFILIATIONS

[1]INFN, Sezione di Firenze, Via Sansone 1, I-50019 Sesto Fiorentino (FI), Italy
[2]European Laboratory for Non-Linear Spectroscopy (LENS), Via Carrara 1, I-50019 Sesto Fiorentino (FI), Italy
[3]CNR-INO, L.go Enrico Fermi 6, I-50125 Firenze, Italy
[4]Dipartimento di Fisica e Astronomia, Università di Firenze, Via Sansone 1, I-50019 Sesto Fiorentino (FI), Italy

[a)]**Author to whom correspondence should be addressed:** marin@fi.infn.it

ABSTRACT

We demonstrate and characterize the transfer of a levitating silica nanosphere between two optical tweezers at low pressure. Both optical traps are mounted on the heads of optical fibers and placed on translation stages in vacuum chambers. Our setup allows us to physically separate the particle loading environment from the experimental chamber, where the second tweezer can position the particle inside a high finesse optical cavity. The separation prevents from spoiling the cavity mirrors and the chamber cleanliness during the particle loading phase. Our system provides a very reliable and simply reproducible protocol for preparing cavity optomechanics experiments with levitating nanoparticles, opening the way to systematic studies of quantum phenomena and easing the realization of sensing devices.

Quantum optomechanics has recently expanded the range of explored and exploited systems to nanoparticles levitating in vacuum, trapped and oscillating in the potential created by an optical field.[1–7] In particular, the topic of cavity optomechanics is very intriguing for the possibility of realizing quantum coupling between the photonic field and the particle motion,[8] where the latter is strongly decoupled from environmental thermal noise by operating in high vacuum.

Most proposals[2–4] and experiments[9–12] aiming to cool the dynamics of a levitating nanoparticle inside an optical cavity are based on the dispersive coupling of its motion to the electromagnetic field, a technique well investigated in optomechanics.[13] A different mechanism of cavity cooling, relying on coherent trapping of light scattered by a levitating nanoparticle into an optical cavity, has been recently realized[14,15] and allowed to achieve motional cooling of a levitated nanoparticle to a phononic occupation number below unity.[16] In any case, accurate positioning of the nanoparticle inside the cavity is crucial to tune and optimize the optomechanical coupling.

To optically trap a neutral nanoparticle, a laser beam is tightly focused in a chamber in the presence of gas containing suspended particles. If their motion is sufficiently damped by collisions with the background gas, trapping occurs as one particle crosses the focused beam and releases its kinetic energy fast enough to be captured by the optical potential. To implement cavity optomechanics experiments, it is then necessary to place the levitating particle into the region defined by a field mode of a high finesse optical cavity with sub-micrometric precision. The position must be stably and accurately maintained, avoiding excess mechanical and acoustic vibrations. A prerequisite loads the dipole trap (optical tweezer) without spoiling the cavity mirrors, something that easily occurs due to particle deposition on the surface of mirrors. Finally, high vacuum conditions must be achieved in reasonable time, maintaining stable conditions. Even this latter procedure is conditioned by the relatively high pressure necessary for the initial trapping stage and often by the presence of solvents used for injecting the particles in the chamber through a nebulizer. A clean and reproducible method to prepare a levitating nanoparticle for cavity optomechanical experiments is actually very useful but not straightforward.

A possibility is to load the particle on the optical tweezer in the first chamber and then transfer it to a cleaner environment containing the optical cavity and the positioner. A movable optical trap is described in Ref. 17. The trap is loaded in the first chamber using

a nebulizer, then the whole tweezer, mounted on micrometric positioners in an extensible arm, is moved to the second chamber, and the particle is delivered to the stationary wave of an optical cavity. To stabilize the particle during the transfer, a cooling scheme acting on the tweezer optical power is used. A different method to transfer a levitating particle between different vacuum chambers is described in Ref. 18. A standing wave is created inside a hollow fiber connecting the two chambers by means of counter-propagating laser beams. The particle is trapped on an anti-node of the standing wave and then moved by slightly shifting the frequencies of the two beams. The collection of the particle in the second chamber has not yet been reported.

In this work, we describe a method for reliably loading a nanoparticle on a stable and accurately positionable tweezer, inside a high finesse optical cavity, avoiding the performance degradation of mirrors. Similar to Ref. 17, the particle is trapped in the first chamber by a tweezer placed on a movable arm and then translated into the experimental chamber containing the optical cavity. It is then transferred to the second optical trap that is mounted inside the second chamber on nano-positioners. This second tweezer is used to accurately position the particle inside the optical cavity. Mounting the nano-positioners on the chamber baseplate that also supports the optical cavity, instead of placing them on the moving arm, significantly improves the overall mechanical stability. Moreover, the moving arm is retracted after the particle transfer, and the vacuum chambers are isolated. As a consequence, the environment in the experiment chamber is suitable for a rapid evacuation down to very low pressure.

The crucial stage in our scheme is the transfer of the nanoparticle between two optical tweezers in a low pressure environment. In the following, we characterize in detail this procedure.

The setup is shown in Fig. 1. Nanoparticles are caught in chamber A and then transferred to the second trap in chamber B. The optical tweezer that captures the particles is realized with a fibered

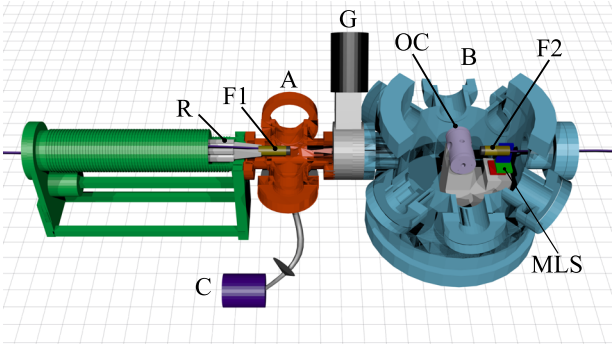

FIG. 1. Experimental setup. Nanoparticles are injected in chamber C and then transported in a gas flux toward chamber A where they are captured by the tightly focused light of a laser diode delivered by a single-mode fiber. The fiber head with the focusing system (F1) is mounted on the tip of a rod (R) that can be manually translated between chambers A and B through the gate G. The second optical tweezer is formed by the light of a Nd:YAG laser and delivered by a similar optical system (F2) mounted on a three-axis miniature linear translation stage (MLS). The focus can be positioned inside the optical cavity (OC) with sub-micrometric precision.

976 nm laser diode (LD). The light delivered by a single-mode fiber is collimated and focused using an optical system (F1) composed of two aspheric lenses, having a nominal focal length and a numerical aperture of 15.4 mm (N.A. 0.16) and 3.1 mm (N.A. 0.68), respectively. The two lenses are screwed on the fiber head connector. The beam at the focus is elliptical with waists of 0.96μm and 0.92μm, as deduced from the particle oscillation frequencies at the typical output power of 250 mW.[19] The fiber head with the optics is mounted at the end of a 500 mm long, X-shape aluminum rod screwed on the moving flange of a bellowed sealed linear shift mechanism (HV Design) that allows us to manually translate it between chambers A and B. We note that this support is sensitive to mechanical vibrations, making this trap unsuitable for stable cavity optomechanics experiments.

A drop of aqueous solution of silica nanospheres (9% of particles, in mass) of radius ~85 nm is injected inside chamber C that is filled with clean nitrogen, while chamber A is evacuated. The valve separating the two chambers is opened, and the dust of nanoparticles is introduced in chamber A, carried by the gas turbulence produced by the pressure unbalance. Trapping by the optical tweezer occurs when a pressure of ~100 mbar is achieved in chamber A, typically within few minutes.

With a particle trapped, before opening the gate G, residual wandering nanoparticles are pumped out from chamber A, whose pressure is gently decreased down to the mbar level. The chamber is then slowly refilled with pure nitrogen up to ~30 mbar, and the gate is opened to equilibrate the pressure between chambers A and B (which was initially in high vacuum). The optical tweezer is translated to chamber B and positioned in front of the second optical trap. We remark that, at this pressure, the nanoparticle motion is over damped, and we can keep the levitating particle during the translation without using any active feedback.

The second tweezer is formed by the 1064 nm radiation of a Nd:YAG laser and delivered into chamber B by a polarization maintaining fiber. The focusing optical system screwed on the fiber head (F2) is the same of the first tweezer and is positioned on a three-dimensional miniature linear stage (PI Q-522). The beam waists at the focus are 1.02μm and 0.93μm, and the typical optical power is 200 mW. Fibered beam-splitters allow us to collect part of the light arriving from the fiber heads. With the help of dichroic mirrors, we can thus measure the transmitted and back-scattered light of both sources.

To transfer the particle between the two tweezers, we have to superpose the positions of their intensity maxima with sub-micrometric precision. This procedure is performed by moving the second fiber head. Its transverse position with respect to the optical axis is optimized by maximizing the light transmission between the two fibers, while the distance between the two fiber heads must take into account the chromatic aberration, as sketched in Fig. 2(b). We remark that the light of the second tweezer remains off during the whole procedure to avoid the accidental formation of an unstable potential by the superposition of the two intensity profiles.

To define the optimization procedure, we have performed a preliminary characterization of the optical coupling between the two fibers at the two used wavelengths. The transmitted power of the Nd:YAG light through the first fiber and that of the LD light through the second fiber are reported in Fig. 2(a). The transverse position of

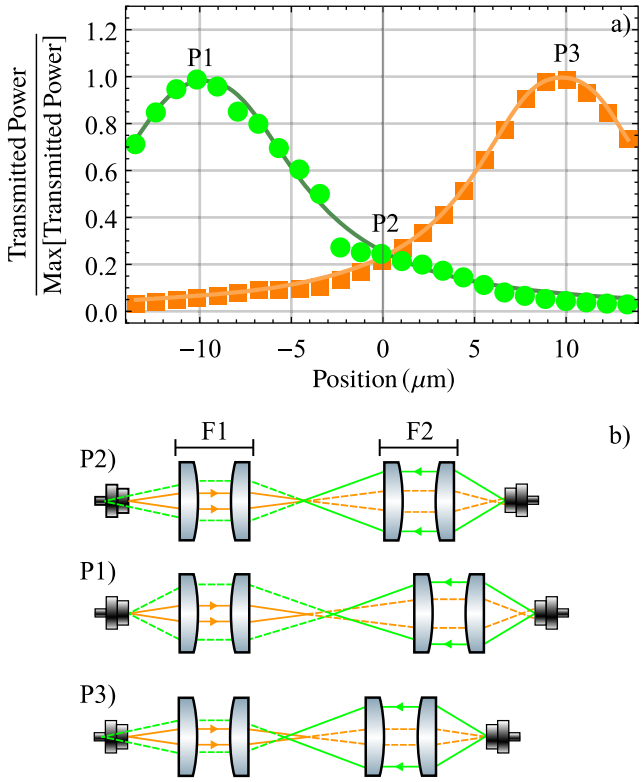

FIG. 2. (a) Transmitted power of the laser light from the two sources through the two optical fibers and the corresponding F1 and F2 optical systems. Green dots: Nd:YAG light. Orange squares: LD light. Data are recorded approaching the two fiber heads at 1.1μm per step and normalized to the maximum transmitted power for each wavelength. Abscissa represents the variation of the distance of the fiber heads with the origin set halfway between the two maxima. Solid lines: overlap integral between the propagating field modes, fitted to the experimental data. (b) Schematic diagram of the two focusing systems during the measurement. Green (orange) rays represent the Nd:YAG (LD) beam propagation with arrows indicating the direction. P2 indicates the optimal position to transfer the particle as the two focuses are spatially overlapped. At relative position P1(P3), the two focusing systems are optimally placed to couple the Nd:YAG (LD) optical power. In that case, the distance between the two traps is 9.8 μm.

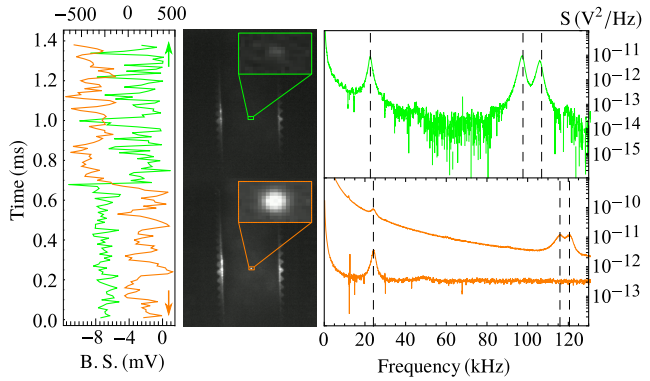

FIG. 3. Left panel: The light back scattered (B.S.) from the particle is collected from the trapping fibers during the transfer between the LD and the Nd:YAG tweezers. Orange: LD light signal (scale on the bottom axis). Green: Nd:YAG light signal (scale on the top axis). Central panel: images of the Nanoparticle trapped by the LD (bottom picture) and the Nd:YAG (top picture) optical tweezers. Bright spots, also shown in the enlarged insets, are due to the particle dipole emission, and scattered light allows us to identify the edges of the focusing lenses. The brightness difference between the two traps is due to the different camera sensitivity at the two wavelengths. Right panel: spectra of the back and forward scattered light, collected by the fibers and acquired at a background pressure of 2 mbar, exhibiting spectral peaks corresponding to the three eigenfrequencies of the particle motion. Bottom graph: spectra of the forward scattering (upper trace) and back scattering (lower trace) of the LD light with the particle on the first tweezer. Top graph: spectrum of the forward scattering of the Nd:YAG light with the particle trapped by the Nd:YAG tweezer. Vertical dashed lines display the particle oscillation frequencies.

the fiber head is kept optimized during the measurement, while the two fiber heads are moved closer at ~ 1.1μm steps. The solid line, for each of the two wavelengths, is given by the overlap integral of the two counter-propagating modes, fitted to the experimental data.

We find a distance of 9.8 μm between the positions of the foci for the two wavelengths. As shown in the scheme of Fig. 2(b), assuming two identical focusing systems, the optimal distance to transfer the particle between the tweezers is halfway between the transmission maxima at the two wavelengths [this position is labeled as P2 in Fig. 2(b)]. The operative procedure is then the following: we optimize the transmission of the LD light through the second fiber by moving the fiber head in the three directions, and afterward, we increase the distance of the fiber heads by ~ 10μm.

To load the second trap, we boost the Nd:YAG power and slowly turn off the LD. With the described protocol, we can reliably transfer the particle between the two traps. In Fig. 3, we show a photo of the two optical systems and the levitating nanoparticle before and after the transfer. The power spectra of the light collected by the fibers in the back and forward directions, also shown in Fig. 3, exhibit the peaks associated with the nanoparticle motion in the three orthogonal directions defined by the trap geometry. In both cases, the background pressure is reduced down to 2 mbar to show such clear signatures of the under-damped motion.

We often observe that the particle scattered light changes suddenly during the transfer. On the other hand, a transfer between potential wells having the same minimal point should be characterized by a continuous change in the apparent particle brightness, following the varying light intensity. The observed abrupt changes indicate that the nanoparticle jumps between two potential minima, which are not perfectly superimposed due to an uncertainty in the positioning of the order of few hundred nanometers and to the optics mechanical vibrations. While turning off the LD, the potential barrier from the first to the second trap as well as the depth of the first trap becomes vanishingly small. To obtain a reliable transfer, the jump rate (favored by the lowering barrier) must be higher enough than the loss rate (increased by the lowering well depth). Moreover, the gas damping must be strong enough to allow the particle losing its kinetic energy during the transfer. Our double tweezer is a versatile system to investigate the stochastic motion of a particle in a variable three-dimensional potential,[20] which is, however, beyond the scope of the present article and is left to further works. At the purpose of providing useful information for the reproduction of our

method, we describe in the following a semi-quantitative investigation of the pressure and misalignment ranges that allow a reliable transfer.

We first characterize the relative mechanical vibrations of the two trapping optics on the plane perpendicular to the optical axis. The two focusing systems are first placed at the position that maximizes the transmitted Nd:YAG power through the two fibers. The transmitted signal is then recorded while moving the second fiber head in the vertical direction. Hence, the fiber head is set at the position that halves the transmitted power, and the time trace of the transmitted signal is acquired and calibrated in terms of displacement fluctuations using the previously recorded transmission curve (as illustrated in the right inset of Fig. 4). The same procedure is repeated for the horizontal displacement. In Fig. 4, we show the calculated displacement noise spectra. The main spectral feature is a double peak at ~50 Hz for the vertical direction, whose area corresponds to a displacement of ~ 50 nm (root mean square), much smaller than the beam waists. A simulation with a finite element model shows that the two peaks are due to flexural modes of the rod that sustains the first fiber head.

In order to define the pressure range that allows a reliable transfer, we have repeated at least three times the transfer back and forth between the two traps at the pressure values of 100 mbar, 75 mbar, 50 mbar, 25 mbar, and 15 mbar. We actually lost the particle during the fourth attempt at 10 mbar. We notice that at 10 mbar the damping rate is about $\Gamma \simeq 2\pi \times 10$ kHz; thus, the particle motion is weakly damped.

At 50 mbar, we have then evaluated the tolerance in the misalignment between the two fiber heads. Starting from the optimal position, we could transfer the particle three times back and forth in different relative positions until the two focuses were misplaced by ~ 3μm on the plane perpendicular to the optical axes or ~ 10μm along the optical axes. For the latter case, we show in Fig. 3, on the left panel, the time evolution of the backscattered light during a transfer from the LD to the Nd:YAG tweezers. The visible steps

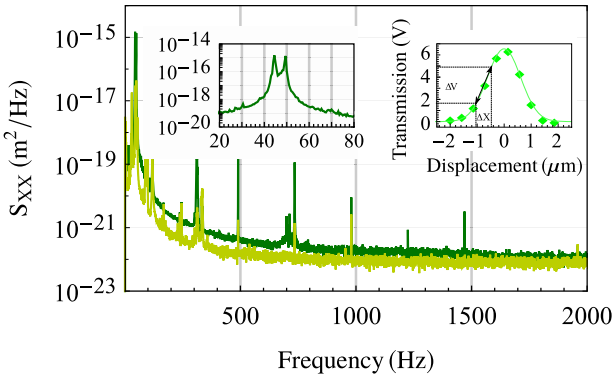

FIG. 4. Spectra of the relative position between the two fiber heads, on the plane perpendicular to the tweezer axis, along the vertical (green) and horizontal (yellow) directions. Left inset: dominant vibrational modes at 44 Hz and 49 Hz in the vertical direction. Right inset: transmitted power of the Nd:YAG light through the two optical fibers, as the second fiber head is translated in the vertical direction. This curve is used to convert into displacement spectra the acquired transmission spectra, as illustrated in the picture.

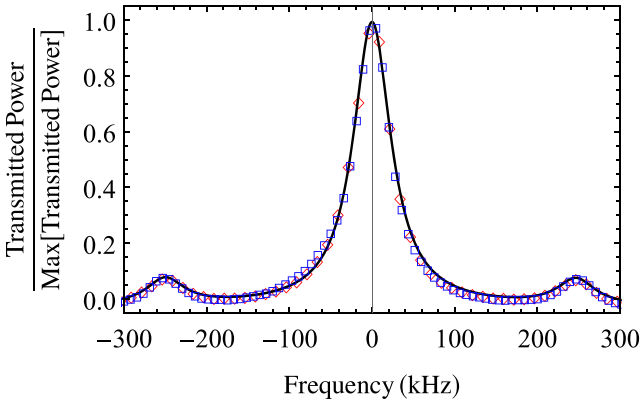

FIG. 5. Transmitted power of a probe Nd:YAG laser through the high finesse optical cavity. Sidebands at ±250 kHz are produced by laser phase modulation for calibrating the frequency scan. The blue squares and red diamonds correspond to acquisitions recorded before the nanoparticle capture and transfer and after ten complete operations, respectively. The solid line shows a fit to the latter dataset.

indicate a jump between the two potential wells occurring in a time shorter than 0.1 ms.

After having defined the above described transfer protocol, we have placed an ~ 50 mm long optical cavity (Finesse 54 000) inside chamber B. The cavity spacer has a 20 mm diameter radial hole that allows us to place on the cavity optical axis the nanoparticle trapped by the Nd:YAG tweezer. We have captured and transferred several particles from the LD to the Nd:YAG trap at a background pressure of 30 mbar and eventually positioned them inside the cavity standing wave. Even after ten complete cycles, we could appreciate no degradation of the cavity finesse, as shown in Fig. 5 where we report two recordings of the cavity transmission function, acquired before the first and after the last transfer operation. The measured width is 57 ± 1 kHz and 56 ± 1.5 kHz, respectively. After the transfer, the arm is moved back, and the science chamber is isolated from the loading chamber and is pumped down to a pressure below 10^{-6} mbar in half an hour.

In conclusion, we have described a robust method to systematically capture and place a levitated nanoparticle with the submicrometric precision inside an optical cavity without spoiling the cavity optical quality and the environment of the experimental chamber. We have, indeed, observed that the optical cavity can be repeatedly loaded without degrading its performance. A key element of our protocol is the transfer of the loaded particle between two completely independent optical tweezers, which we realize and characterize and which is performed without the necessity of stabilizing feedback loops. Hence, the second tweezer can be mounted on stable nano-positioners, which allows a reliable and systematic investigation of the coupling between the nanoparticle and the cavity optical field. Our system provides a very reliable and simply reproducible protocol for preparing cavity optomechanics experiments with levitating nanoparticles, opening the way to systematic studies of quantum phenomena and easing the realization of sensing devices.[21]

We thank A. Pontin for assistance at the early stage of this work. This research was performed within the Project QuaSeRT

funded by the QuantERA ERA-NET Cofund in Quantum Technologies implemented within the European Union's Horizon 2020 Programme.

DATA AVAILABILITY

The data that support the findings of this study are available from the corresponding author upon reasonable request.

REFERENCES

[1] A. Ashkin, Proc. Natl. Acad. Sci. U. S. A. **94**, 4853 (1997).
[2] D. E. Chang, C. A. Regal, S. B. Papp, D. J. Wilson, J. Ye, O. Painter, H. J. Kimble, and P. Zoller, Proc. Natl. Acad. Sci. U. S. A. **107**, 1005 (2010).
[3] P. F. Barker and M. N. Shneider, Phys. Rev. A **81**, 023826 (2010).
[4] O. Romero-Isart, M. L. Juan, R. Quidant, and J. I. Cirac, New J. Phys. **12**, 033015 (2010).
[5] T. Li, S. Kheifets, and M. G. Raizen, Nat. Phys. **7**, 527 (2011).
[6] J. Gieseler, B. Deutsch, R. Quidant, and L. Novotny, Phys. Rev. Lett. **109**, 103603 (2012).
[7] J. Millen, T. S. Monteiro, R. Pettit, and A. N. Vamivakas, Rep. Prog. Phys. **83**, 026401 (2020).
[8] O. Romero-Isart, A. C. Pflanzer, M. L. Juan, R. Quidant, N. Kiesel, M. Aspelmeyer, and J. I. Cirac, Phys. Rev. A **83**, 013803 (2011).
[9] N. Kiesel, F. Blaser, U. Delic, D. Grass, R. Kaltenbaek, and M. Aspelmeyer, Proc. Natl. Acad. Sci. U. S. A. **110**, 14180 (2013).
[10] P. Asenbaum, S. Kuhn, S. Nimmrichter, U. Sezer, and M. Arndt, Nat. Commun. **4**, 2743 (2013).
[11] J. Millen, P. Z. G. Fonseca, T. Mavrogordatos, T. S. Monteiro, and P. F. Barker, Phys. Rev. Lett. **114**, 123602 (2015).
[12] N. Meyer, A. de los Rios Sommer, P. Mestres, J. Gieseler, V. Jain, L. Novotny, and R. Quidant, Phys. Rev. Lett. **123**, 153601 (2019).
[13] M. Aspelmeyer, T. J. Kippenberg, and F. Marquardt, Rev. Mod. Phys. **86**, 1391 (2014).
[14] D. Windey, C. Gonzalez-Ballestero, P. Maurer, L. Novotny, O. Romero-Isart, and R. Reimann, Phys. Rev. Lett. **122**, 123601 (2019).
[15] U. Delić, M. Reisenbauer, D. Grass, N. Kiesel, V. Vuletic, and M. Aspelmeyer, Phys. Rev. Lett. **122**, 123602 (2019).
[16] U. Delić, M. Reisenbauer, K. Dare, D. Grass, V. Vuletić, N. Kiesel, and M. Aspelmeyer, Science **367**, 892 (2020).
[17] P. Mestres, J. Berthelot, M. Spasenović, J. Gieseler, L. Novotny, and R. Quidant, Appl. Phys. Lett. **107**, 189901 (2015).
[18] D. Grass, J. Fesel, S. G. Hofer, N. Kiesel, and M. Aspelmeyer, Appl. Phys. Lett. **108**, 221103 (2016).
[19] L. Novotny and B. Hecht, *Principles of Nano-Optics* (Cambridge University Press, Cambridge, England, 2012).
[20] L. Rondin, J. Gieseler, F. Ricci, R. Quidant, C. Dellago, and L. Novotny, Nat. Nanotechnol. **12**, 1130 (2017).
[21] G. Ranjit, M. Cunningham, K. Casey, and A. A. Geraci, Phys. Rev. A **93**, 053801 (2016).